Aircraft High-Lift Aerodynamic Analysis Using a Surface-Vorticity Solver

Erik D. Olson[*] and Cindy W. Albertson[†]

NASA Langley Research Center, Hampton, VA 23681

This study extends an existing semi-empirical approach to high-lift analysis by examining its effectiveness for use with a three-dimensional aerodynamic analysis method. The aircraft high-lift geometry is modeled in Vehicle Sketch Pad (OpenVSP) using a newly-developed set of techniques for building a three-dimensional model of the high-lift geometry, and for controlling flap deflections using scripted parameter linking. Analysis of the low-speed aerodynamics is performed in FlightStream, a novel surface-vorticity solver that is expected to be substantially more robust and stable compared to pressure-based potential-flow solvers and less sensitive to surface perturbations. The calculated lift curve and drag polar are modified by an empirical lift-effectiveness factor that takes into account the effects of viscosity that are not captured in the potential-flow solution. Analysis results are validated against wind-tunnel data for The Energy-Efficient Transport AR12 low-speed wind-tunnel model, a 12-foot, full-span aircraft configuration with a supercritical wing, full-span slats, and part-span double-slotted flaps.

I. Introduction

TAKEOFF and landing performance requirements often have a strong influence on the size of the wing and engines during conceptual aircraft design, yet the low-speed aerodynamic characteristics of an aircraft with its flaps deflected can be difficult to estimate accurately. In particular, the maximum lift coefficient is a difficult value to obtain accurately, even when comprehensive information about the high-lift geometry is available and the configuration is analyzed using higher-order analysis methods.[1,2] Traditionally, designers have tended to rely on scaling of available historical data and test results,[3] but these are of limited use with newer unconventional configurations for which no full-scale data are available.

In a previous study we demonstrated the utility of a semi-empirical approach to high-lift analysis using a vortex-lattice analysis combined with empirical relationships for lift effectiveness that account for non-linear effects such as large deflection angles and viscosity.[4] The vortex-lattice analysis is valid for conventional aircraft configurations, but it may be desirable to use a three-dimensional potential flow solution for some unconventional aircraft, such as a blended wing-body or double-bubble fuselage, or for aircraft with low-aspect-ratio or highly-swept wings. In addition, a three-dimensional analysis potentially enables the use of the pressure-difference rule for prediction of maximum lift coefficient; this simple semi-empirical approach has been shown to be effective at predicting the stall of both clean and multi-section wings.[5]

This study extends the existing semi-empirical approach to examine its effectiveness for use with a three-dimensional aerodynamic analysis of the high-lift configuration. In addition to improved validity for unconventional configurations, the ability to predict the full flow field around the high-lift components opens up additional degrees of freedom that can enable the designer to optimize both the geometry and the deflections of the high-lift system for the particular application. This capability allows a full systems-level design of the high-lift system rather than simply relying on typical performance data for existing systems.

---

[*]Aerospace Engineer, Aeronautics Systems Analysis Branch, Senior Member AIAA.
[†]Aerospace Engineer, Vehicle Analysis Branch.

American Institute of Aeronautics and Astronautics

II.   Methodology

The methodology begins with a parametric model of the geometry in Vehicle Sketch Pad (OpenVSP)[6] to define the outer mold line of the aircraft. A computational grid is exported from OpenVSP and used to perform an aerodynamic analysis in the FlightStream[7] vorticity-based potential-flow solver. The modeling techniques used are described in the following sections.

A.   Modeling of High-Lift Geometry in OpenVSP

OpenVSP is a parametric geometry modeler that has been used extensively for conceptual design studies of aircraft. OpenVSP lacks a built-in capability for directly modeling the high-lift components (main wing, slat, vane and flap), but this study makes use of a newly-developed set of techniques for utilizing OpenVSP's existing capabilities to build a three-dimensional model of the high-lift geometry, and for controlling flap deflections using scripted parameter linking.[8] In this methodology, the components of the high-lift configuration are modeled as separate wing-like surfaces, using airfoil coordinates that are a fraction of the chord of the full wing (Fig. 1). Since OpenVSP does not allow discontinuities in the spanwise arrangement of cross sections, additional short transition segments are inserted into the main wing surface to allow for a nearly-discontinuous change between adjacent segments with and without flaps (Fig. 2). These transition segments allow the main component to be modeled as a continuous surface with only a minor loss of fidelity due to the finite spanwise length of the transition segments; however, their use has the disadvantage of causing highly-skewed triangles in the exported grid. As a result, the transition segments require special handling in the flow solution, as described in Section II.B.
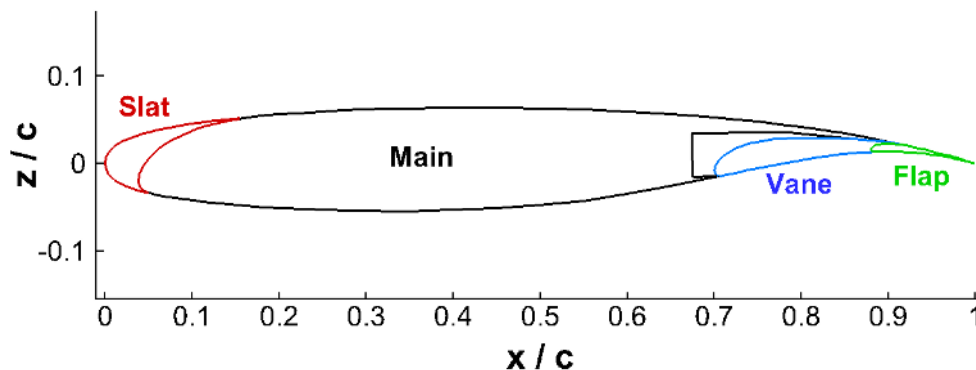

Figure 1.   Airfoil coordinates for a wing with slat and double-slotted flaps

Once the high-lift components have been modeled and the flaps and slats have been moved to their deployed positions, OpenVSP performs a simple intersection of the components and inserts diagonals into quadrilateral panels to produce a water-tight surface mesh of triangular panels (Fig. 3), which is then exported in the 3D Systems[TM] stereolithography (STL) file format. This quick triangulation tends to produce highly-skewed triangles in the vicinity of the intersection curves. OpenVSP is also capable of producing a high-quality surface mesh of nearly isotropic triangles, but the aerodynamic analysis has been found to work acceptably well with the simple mesh,[9] which can be produced in a fraction of the time; therefore, the simple intersection routine is used here, with no attempt to further improve the quality of the triangles.

B.   Aerodynamic Analysis

Analysis of the aerodynamics of the high-lift configurations is performed in FlightStream, a novel surface-vorticity solver capable of using structured or unstructured surface meshes. As a vorticity-based solver, the code can be expected to be substantially more robust and stable compared to pressure-based potential-flow solvers and less sensitive to surface perturbations; and it also allows the use of coarser meshes with an acceptable level of fidelity. The code uses an unstructured wake-strand model to handle wakes emanating from unstructured meshes. The analysis is inviscid, with a separate prediction of the skin-friction drag based on the surface vorticity.
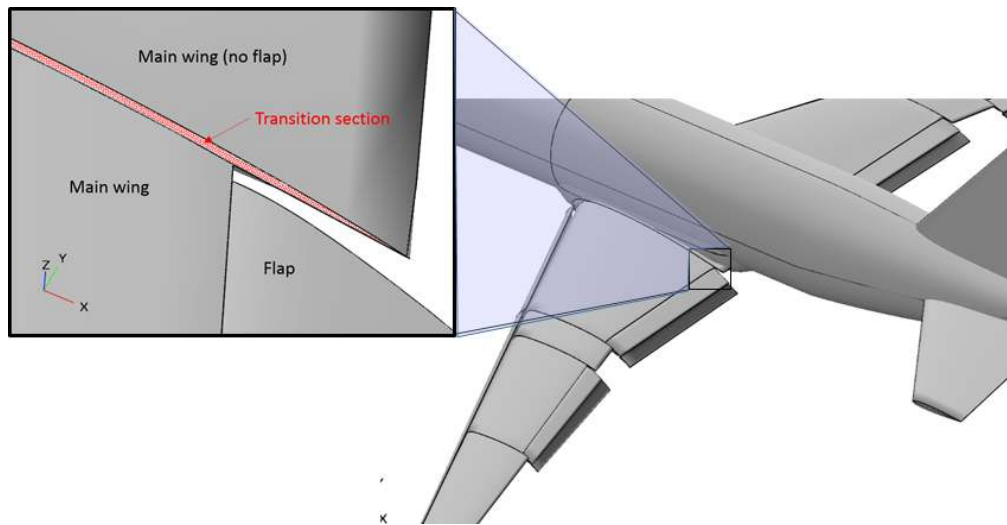
American Institute of Aeronautics and Astronautics

Figure 2. Transition section between flapped and unflapped segments of the main wing component
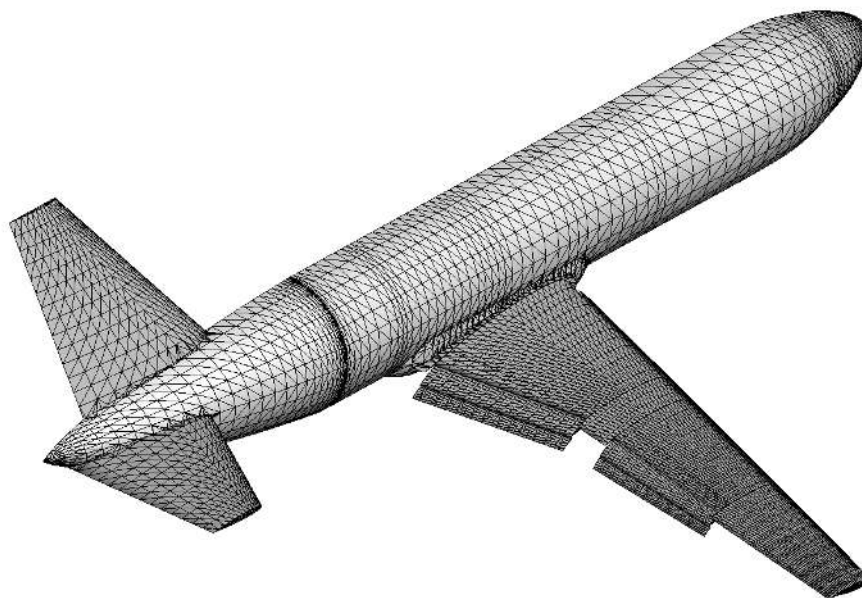
Figure 3. Intersected and triangulated geometry exported from OpenVSP

American Institute of Aeronautics and Astronautics

FlightStream has the ability to read geometry in the STL format, so importing the geometry created by OpenVSP is straightforward. However, even though FlightStream is fairly insensitive to grid density, some modification of the input geometry is required to improve convergence of the solution. In particular, numerical instabilities can occur when two adjacent panels are very different in size, or if the aspect ratio of a panel is extremely large. The following modifications to the imported geometry are typically required in order to improve the convergence:

- Remove the transition sections between flapped and unflapped sections; these are much smaller than the wing panels that are immediately adjacent (Fig. 4).

- Remove the tip caps used to close up the ends of the wing components; these are also much smaller than adjacent panels (Fig. 4).

- Remove the last several rows of panels in the lower surface of the flap near the trailing edge. Due to the extreme thinness of the airfoil in this location, the upper- and lower-surface panels have nearly the same influence coefficients and boundary conditions, and including both results in a poorly-posed problem.

- Remove panels in the slat, flap and vane cove regions (Fig. 5). Since the flow is expected to be massively separated in these regions, it is not valid to enforce a flow tangency condition on these panels.

- Remove any extremely high-aspect-ratio triangles in the immediate vicinity of the trailing edges of the wing-body and tail-body intersection regions; these triangles tend to cause instabilities in the Kutta condition.

Since FlightStream is a panel code without a volume grid, it is not necessary that the computational geometry be watertight, so the analysis can be performed with some of the panels removed. The removed panels generally have a negligible effect on the solution because they are very small, or because they are in regions that do not contribute significantly to the integrated aerodynamic loads.
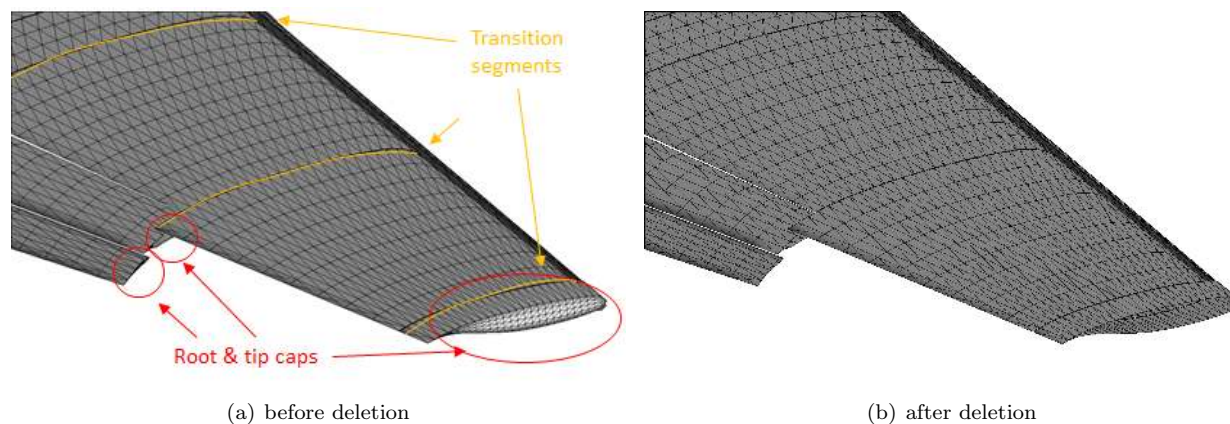

(a) before deletion   (b) after deletion

Figure 4. FlightStream computational grid before and after deletion of tip caps and transition segments

As a final step in preparing the computational grid, it is necessary to designate trailing edges where the Kutta condition will be applied. FlightStream can do this automatically, or the edges can be designated manually.

When the model is finalized, FlightStream automatically removes the diagonals that were inserted into quadrilateral panels in OpenVSP, converting them back to the original quadrilaterals. This step greatly improves the efficiency of the solution by cutting the number of panels nearly in half. Once these steps have been performed, the computational model is ready for analysis (Fig. 6).

C. Empirical Lift Effectiveness

In practice, the flap lift increment cannot accurately be predicted by inviscid analysis because of several viscous effects. First, the de-cambering effect of the boundary layer near the trailing edge of the flap results
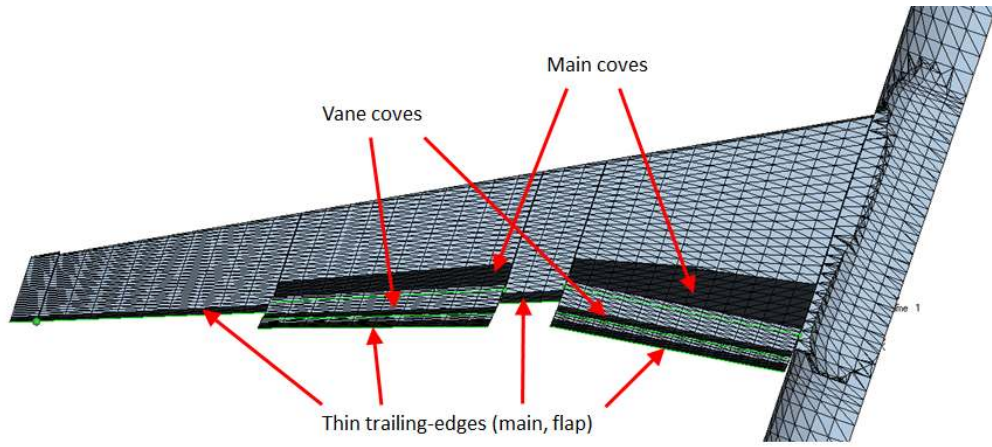
American Institute of Aeronautics and Astronautics

Figure 5. FlightStream computational grid with coves and lower-surface trailing-edge regions removed
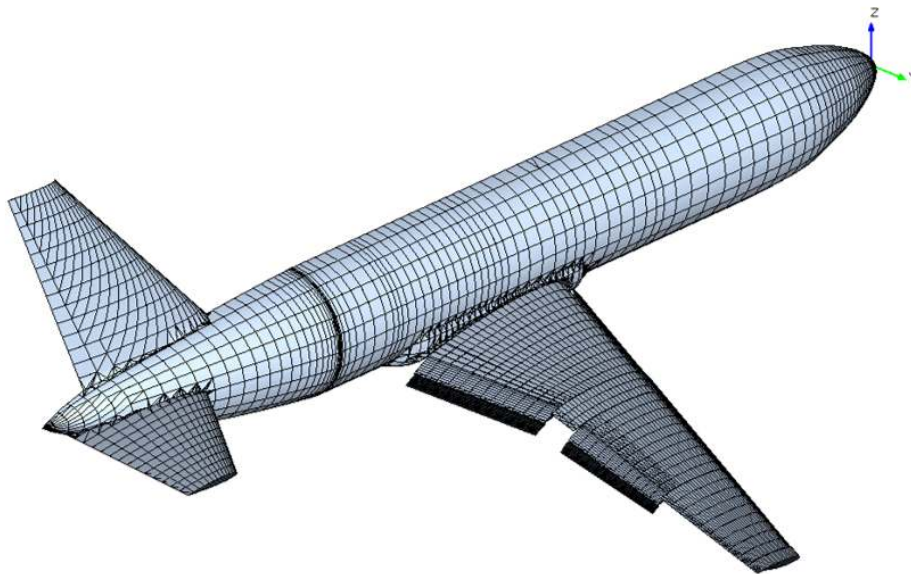
Figure 6. FlightStream computational model

American Institute of Aeronautics and Astronautics

in a smaller lift coefficient than predicted.[10] Second, at large flap angles the flow can become separated. These effects are captured using an empirical flap effectiveness factor, η, which is applied as a multiplier to the calculated lift increment. The flap effectiveness factor was previously found to give a good estimate of the flap lift increment when combined with a vortex-lattice analysis,[4] and in this study it is applied to the three-dimensional analysis for comparison.

Figure 7 shows empirical curves of flap effectiveness factor for various types of flap systems as a function of deflection angle. The curves are similar to the effectiveness factors used in the previous study, except that they are referenced to a three-dimensional potential-flow solution and do not include the additional correction for large flap angles that is required for a vortex-lattice analysis.
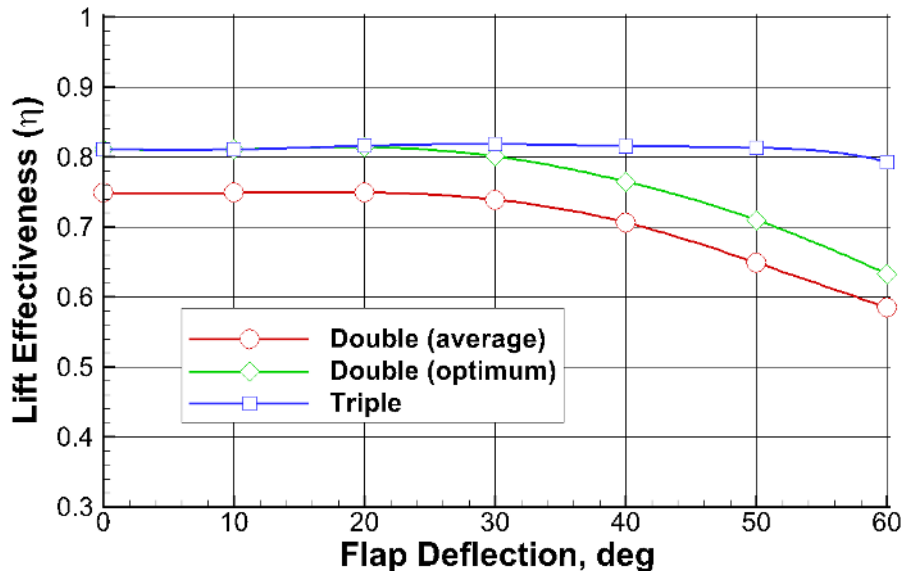

Figure 7. Empirical lift effectiveness for double- and triple-slotted flaps as a function of deflection angle, relative to three-dimensional inviscid analysis. *Source:* **data from Ref. 11.**

III. Validation

The Energy-Efficient Transport (EET) AR12 low-speed wind-tunnel model[12, 13] was used as a validation case for the aerodynamic analysis methodology (Fig. 8). This model is a 12-foot, full-span aircraft configuration with a supercritical wing, full-span slats, and part-span double-slotted flaps with a cutout for the engine (Fig. 9). In some of the test cases, the model was equipped with flow-through nacelles and landing gear, as in the image, but in this study the validation was carried out for the cases in which they were removed.

A. OpenVSP Model

An OpenVSP model of the EET AR12 has been constructed using the published planform shape, airfoil coordinates, twist distribution, and fuselage cross-section shapes. The slat, vane, flap, and main component geometries were modeled using the published airfoil coordinates and the modeling strategies described in Section II.A. Further details on the modeling of this configuration in OpenVSP are given in Ref. 8.

The flap positions for this configuration are given in Table 1 in terms of the relative positions—gap and overlap (normalized by chord) and relative deflection—for the two high-lift cases of interest; Figure 10 shows how these parameters are defined. The *gap* is the minimum distance from the upper surface of the aft component to the lower-surface trailing-edge point on the forward component. The *overlap* is defined as the distance from the lower-surface trailing edge of the forward component to the forward-most point on the aft component, measured parallel to the longest chord line of the forward component. Finally, the *relative deflection* (δ_s, δ_v, and δ_f for the slat, vane and flap, respectively) is the angle between the longest chord lines of the forward and aft components.

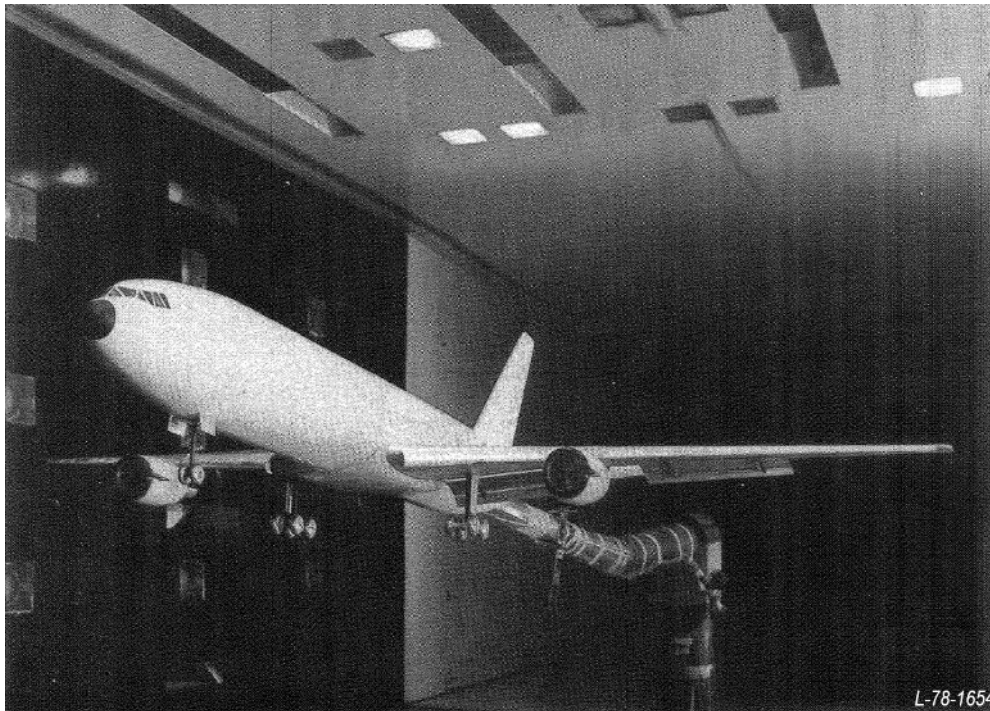American Institute of Aeronautics and Astronautics

Figure 8. EET AR12 model in the NASA-Langley 14x22 wind tunnel. *Source*: Ref. 12

Table 1. Gap, overlap and relative deflection for EET AR12. *Source*: Ref. 12

Configuration	Component	Gap/c	Overlap/c	Rel. Defl., deg
Takeoff	Slat	0.02	0.02	50
	Vane	0.015	0.04	15
	Flap	0.01	0.01	15
Landing	Slat	0.02	0.02	50
	Vane	0.02	0.03	30
	Flap	0.01	0.005	30

American Institute of Aeronautics and Astronautics

Leading-edge slat   15.5-percent c

Inboard double-   Constant chord
slotted flap   30-percent c
                    at η = 0.383

Outboard double-   30-percent c
slotted flap

High-speed aileron 30-percent c

Low-speed aileron   30-percent c

Ground spoilers   Constant chord
                    L.E. 78.5-percent c,
                    T.E. 90-percent c
                    At η = 0.383

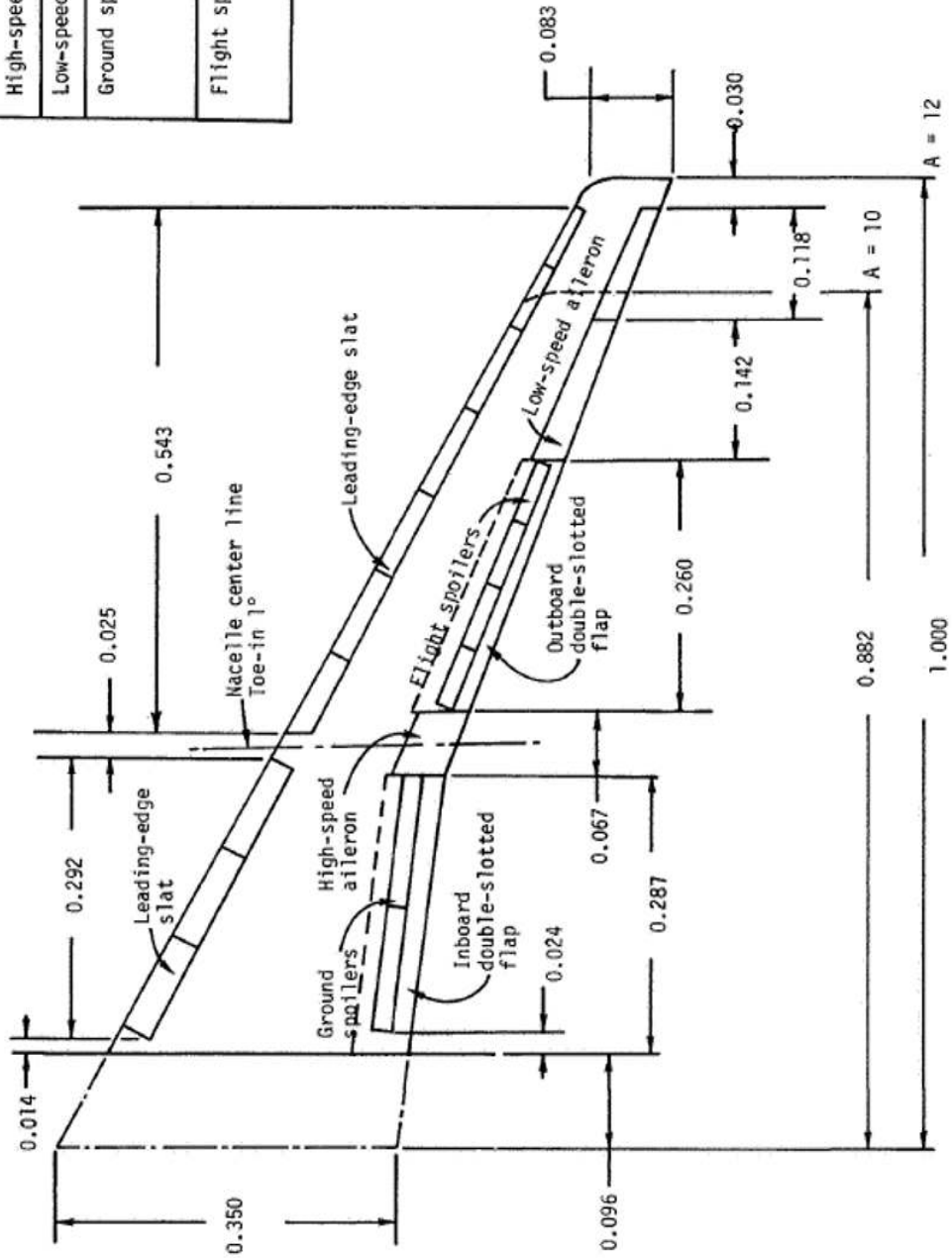Flight spoilers   11.5-percent c
                    L.E. 78.5-percent c
                    T.E. 90-percent c

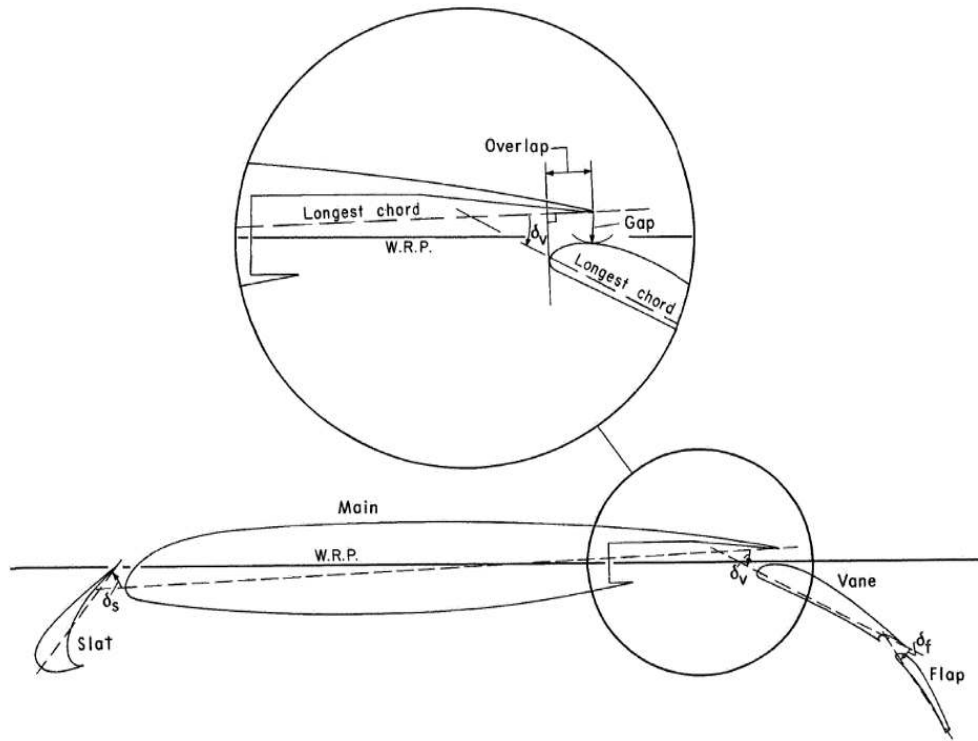Figure 9. EET AR12 model planform detail. *Source*: Ref. 12

American Institute of Aeronautics and Astronautics

Figure 10. Definition of gap, overlap, and deflection (δ). *Source*: **Ref. 12**

The gap, overlap and relative deflection were calculated by post-processing the exported geometry, and the translations and rotation of each component in the OpenVSP model were adjusted by an optimizer to produce the correct relative positioning at both the inboard and outboard locations. Further details of this process are given in Ref. 8. Figure 11 shows the final OpenVSP model of the EET AR12 configuration for the cruise configuration (no flaps and slats modeled), and for the takeoff and landing flap settings.

B.   Analysis Results

FlightStream has the option of performing the analysis using either a prescribed or free-wake propagation model. With a prescribed wake, the wake strands convect downstream with the freestream velocity, including the effects of angle of attack, but are not influenced by the vorticity of the surface panels, or each other. With a free wake, the wake strands are influenced by the vorticity of the solution and follow the local flow direction, resulting in roll-up at the wing tips (Fig. 12). The prescribed wake solution can be performed at a fraction of the time (approximately 20%) and converges easily, whereas the free wake solution is more computationally intensive but may capture near-field wake effects more accurately.

Deflection of slats and slotted flaps results in a large number of interactions between adjacent surfaces (slat/main, main/vane and vane/flap), with the wakes of the upstream components passing in close proximity to the downstream surface. When using a free wake, it was necessary to greatly reduce the wake strand step size to allow the solution to properly trace the curvature of the wake in these high-gradient regions, and to aid in the convergence. The small step size, in turn, caused a significant increase in the solution time.

It was also not possible to use wake separation for the slat. In the prescribed-wake cases, the slat wake passes directly through the main wing surface, while in the free-wake cases the solution was not able to achieve convergence of the slat wake path in close proximity to the main component surface. For these reasons, the slat was removed from the model prior to the analysis. Since the slat would be expected to have no net effect on the lift,[14] using a non-lifting slat surface should not hurt the accuracy of the lift curve and should also not have a large impact on the drag calculation.

American Institute of Aeronautics and Astronautics
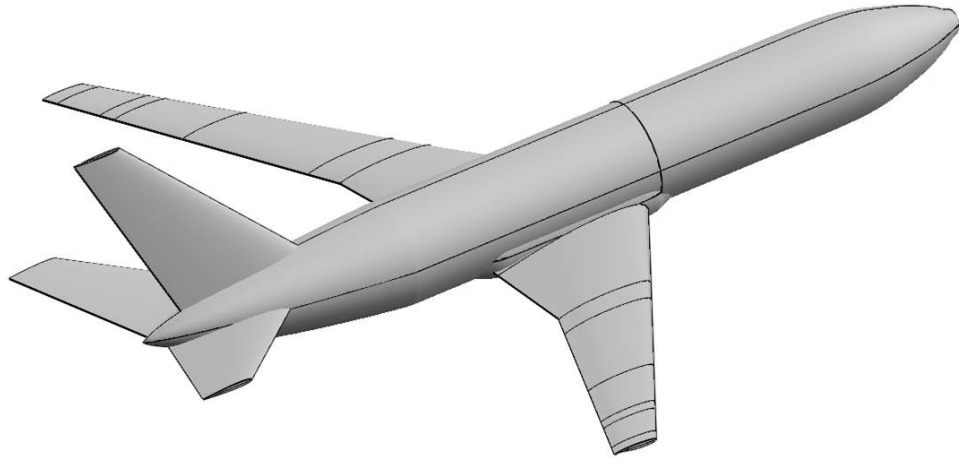
(a) Cruise configuration
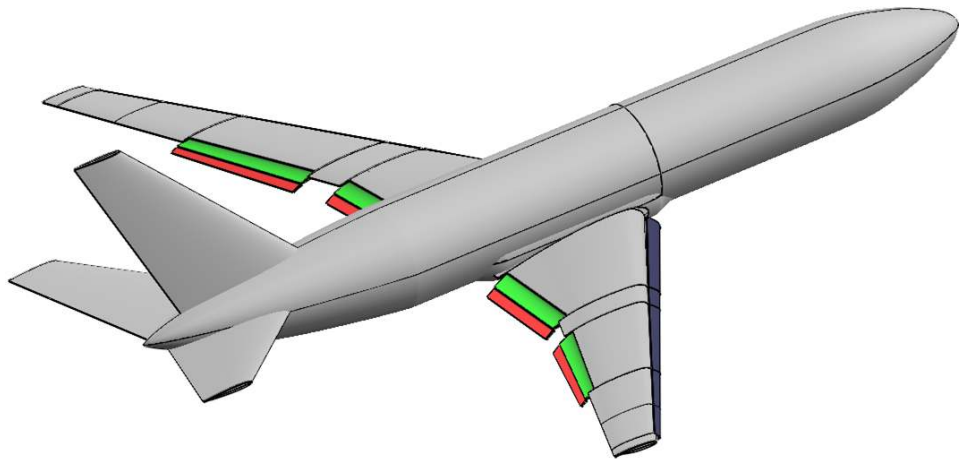
(b) Takeoff flaps
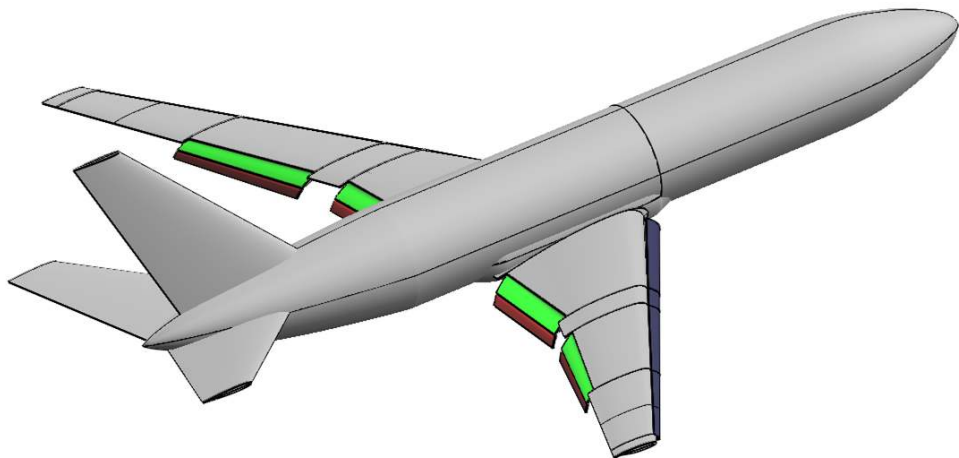
(c) Landing flaps

Figure 11. EET AR12 model with direct flap modeling

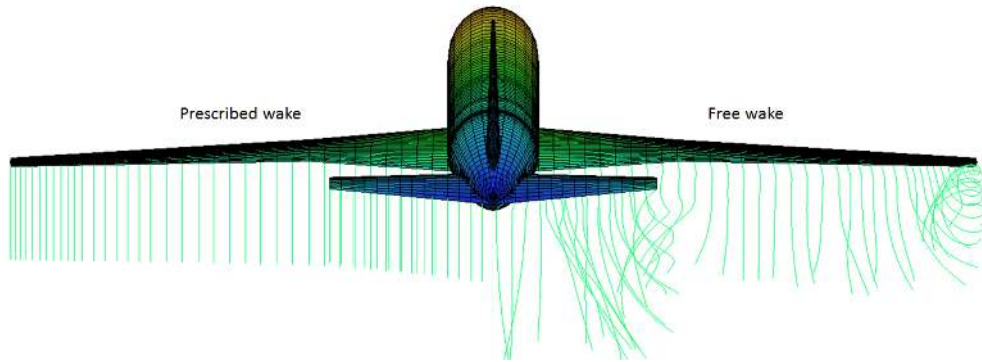American Institute of Aeronautics and Astronautics

Figure 12. FlightStream wake behavior, prescribed vs. free wake

1. Prescribed vs. Free Wake

An initial set of cases were run to determine whether the analysis could be performed accurately with the prescribed wake, or whether it was necessary to incur the extra computational expense of the free wake. Analyses were performed for the cruise and takeoff configurations for both wake options. Figure 13(a) shows the results for the cruise configuration. There is not a significant difference between the lift curves in the two cases; the induced drag, however, is as much as 25% lower at higher angles of attack, although at angles of attack below the stall the difference is less.

Figure 13(b) shows the results for the takeoff configuration. Since FlightStream is a potential-flow analysis and does not account for the effects of viscosity on the lift increment, the results have been augmented with "corrected" data that multiplies the lift increment (the difference between the lift coefficient in the cruise and takeoff configurations) by the lift effectiveness factor, $\eta = 0.80$, which is taken from Fig. 7 for an optimized double-slotted flap.

Once again there is not a significant difference between the lift curves for a prescribed vs. free wake, although the prescribed-wake case can be seen to exhibit a smoother lift-curve slope due to its more robust convergence. Again, the induced drag is lower for the free wake case, and the lift and drag curves for the corrected free-wake analysis compare favorably with the experimental data at moderate to high angles of attack. In the experimental data there is an unexpectedly low lift increment and non-linearity in the lift curve at near-zero angles of attack, suggesting that the combination of takeoff flap geometry and deflection was not particularly ideal at those test conditions; as a result, a firm conclusion cannot be made about the validity of FlightStream's lift and drag results at those conditions.

Overall, these comparisons demonstrate that the free-wake option is necessary to accurately model the drag polar, particularly with flaps deflected. The potential-flow lift increment is also seen to be optimistic and needs to be corrected to account for viscous effects.

2. Comparison to Experiment

Analysis results for EET AR12 model using a semi-empirical correction to the Athena Vortex-Lattice (AVL) method were published previously.[4] Figure 14 shows the FlightStream analysis results compared to both the previous AVL results and the wind-tunnel data. A free-wake solution for the takeoff flap setting is shown in Fig. 14(b) both with and without the empirical correction factor of 80%. Free-wake results are not available for the landing configuration, but the prescribed-wake results are shown for comparison in Fig. 14(c), with and without a 63% correction factor corresponding to the 60° flap deflection.

FlightStream results for the lift curve compare favorably to the data and are similar to the AVL results, which also use empirical corrections to a potential-flow analysis. The drag polar for takeoff compares favorably with the data at moderate angles of attack and is improved over the vortex-lattice results. Although free-wake landing results are not available, the prescribed-wake results are also similar to the AVL results for the lift curve; the shape of the drag polar is improved at moderate angles of attack, and it is expected that the induced drag will decrease for a free-wake solution and be more in line with the experimental data.

In both high-lift cases, the zero-lift drag seems to be under-predicted. Some of this under-prediction can be explained by the lack of slat drag in the FlightStream model. The analysis also lacks a prediction of the

American Institute of Aeronautics and Astronautics
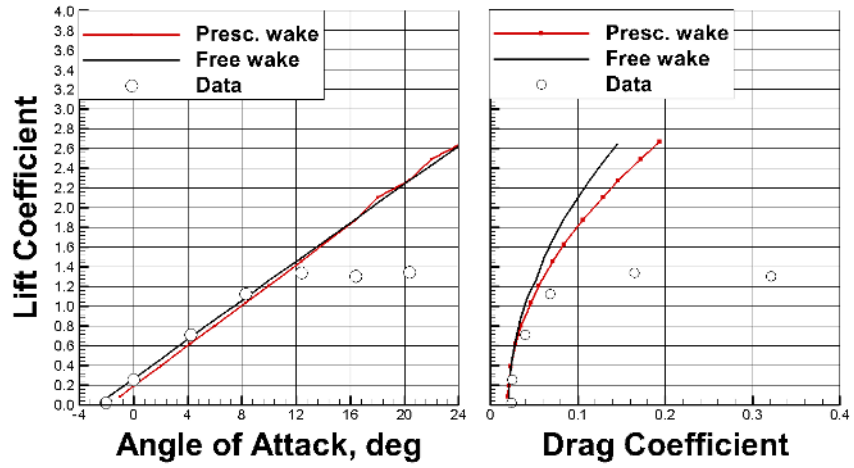
(a) Cruise wing
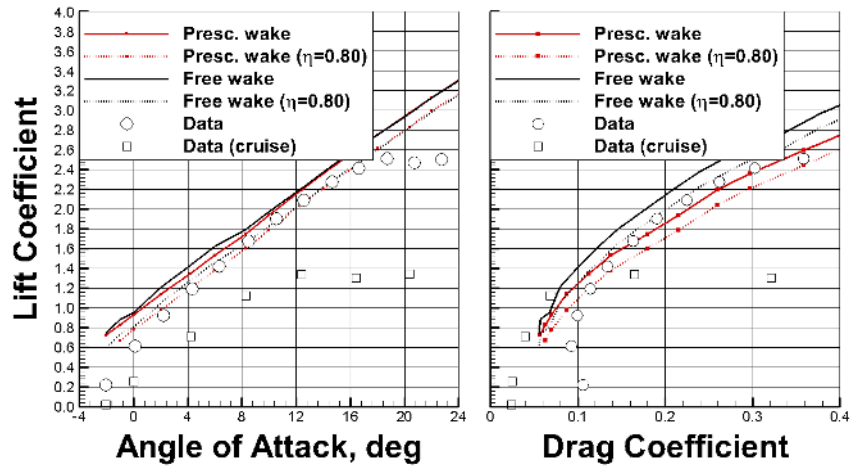
(b) Takeoff flaps, $\delta_s = 50°$, $\delta_f = 30°$

Figure 13. FlightStream analysis results with prescribed vs. free wakes—EET AR12 model, Mach 0.168, $Re_c = 1.37 \times 10^6$

American Institute of Aeronautics and Astronautics

base drag of the massively-separated cove regions, adding an additional correction for the base drag in these regions could further improve the drag prediction.

IV.   Conclusion

In this study, the existing semi-empirical aerodynamic analysis for high-lift configurations was extended to include a three-dimensional analysis using a novel vorticity-based potential-flow method, which is expected to be more robust and stable compared to pressure-based potential-flow solvers and less sensitive to surface perturbations, while also allowing the use of coarser meshes with an acceptable level of fidelity. Extending the analysis to three dimensions makes the process more valid for configurations where thickness effects are important, such as a blended wing-body or double-bubble fuselage.

Free-wake solutions in FlightStream did not have a significant effect on the calculated lift curves, but were found to be necessary for accurate induced-drag calculations at moderate to high angles of attack. Due to the large number of interactions between adjacent surfaces (slat/main, main/vane and vane/flap) and high velocity gradients in those regions, it was necessary to greatly reduce the wake strand step size to aid in the convergence. The small step size, in turn, caused a significant increase (a factor of over 3.8) in the solution time.

In addition, it was necessary to turn off wake separation for the slat in order to achieve convergence of the solution; since the slat would be expected to have no net effect on the lift, using a non-lifting slat surface should not hurt the accuracy. However, the slat does affect the maximum lift of the configuration and so it will be necessary to include the slat wake in the future if stall calculations are added. Efforts are currently underway to adopt an adaptive wake strand step size model, which should improve convergence in the high-gradient regions around the high-lift components, as well as improve overall solution efficiency by using small wake step sizes only where they are needed.

Since FlightStream is a potential-flow analysis method, it does not account for the effects of viscosity on flap lift effectiveness, which can be significant. As a result, the lift increments calculated by FlightStream were expected to be optimistic, and this was demonstrated in the results. Applying the empirical flap effectiveness factors was found to be necessary in order to more-accurately predict the real-world lift and drag performance of the flap system, particularly at large deflections. The zero-lift drag prediction might also be improved in FlightStream by including a base-drag calculation for the massively-separated cove regions.

Overall, the analysis results are consistent with the previous results using lower-order analysis. Due to its speed, robustness and insensitivity to grid density, it is anticipated that the FlightStream analysis could be a key component in a high-lift design and optimization process that will allow designers to investigate tradeoffs between improved aerodynamic performance and increased system complexity and weight.

Acknowledgments

References

[1]Rumsey, C. L., Slotnick, J. P., Long, M., Stuever, R. A., and Wayman, T. R., "Summary of the First AIAA CFD High-Lift Prediction Workshop," *Journal of Aircraft*, Vol. 48, No. 6, 2011, pp. 2068–2079.

[2]Rumsey, C. L. and Slotnick, J. P., "Overview and Summary of the Second AIAA High-Lift Prediction Workshop," *Journal of Aircraft*, Vol. 52, No. 4, 2015, pp. 1006–1025.

[3]Raymer, D. P., *Aircraft Design: A Conceptual Approach*, AIAA Education Series, Washington, DC, 1989.

[4]Olson, E. D., "Semi-Empirical Prediction of Aircraft Low-Speed Aerodynamic Characteristics," *53rd AIAA Aerospace Sciences Meeting*, AIAA, Kissimmee, FL, 2015.

[5]Valarezo, W. O. and Chin, V. D., "Method for the Prediction of Wing Maximum Lift," *Journal of Aircraft*, Vol. 31, No. 1, 1994, pp. 103–109.

[6]Hahn, A., "Vehicle Sketch Pad: A Parametric Geometry Modeler for Conceptual Aircraft Design," *48th AIAA Aerospace Sciences Meeting Including the New Horizons Forum and Aerospace Exposition*, AIAA 2010-657, Orlando, FL, 2010.

[7]Ahuja, V., *Aerodynamic Loads Over Arbitrary Bodies by Method of Integrated Circulation*, Ph.D. thesis, Auburn University, Auburn, AL, Aug. 2013.
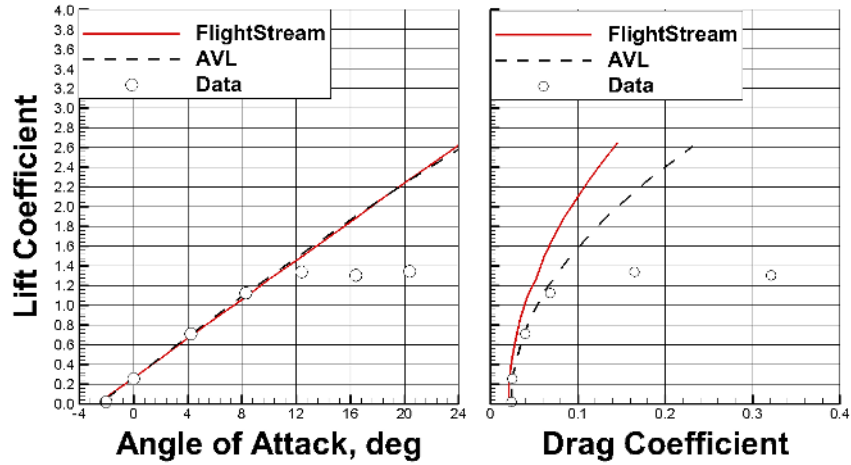
(a) Cruise wing
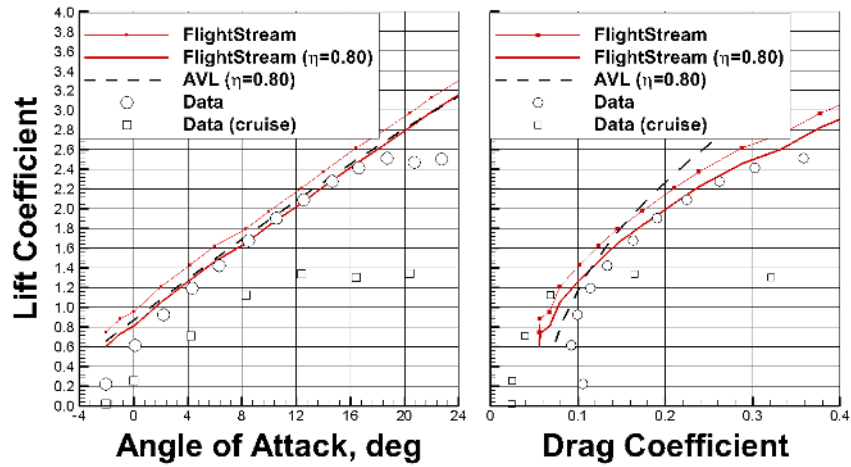
(b) Takeoff flaps, $\delta_s = 50°$, $\delta_f = 30°$
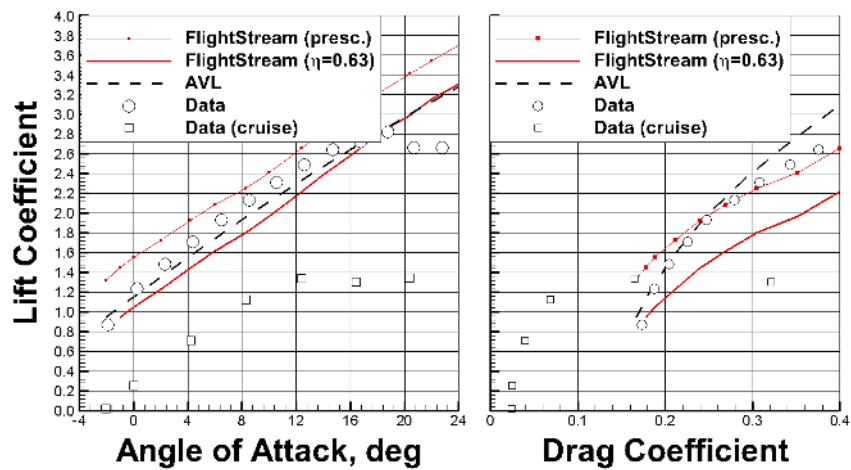
(c) Landing flaps, $\delta_s = 50°$, $\delta_f = 60°$

Figure 14. Analysis results—EET AR12 model, Mach 0.168, $Re_c = 1.37 \times 10^6$

American Institute of Aeronautics and Astronautics

[8]Olson, E. D., "Three-Dimensional Modeling of Aircraft High-Lift Components with Vehicle Sketch Pad," *54th AIAA Aerospace Sciences Meeting*, AIAA, San Diego, CA, 2016.

[9]King, L., Hartfield, R. J., and Ahuja, V., "Aerodynamic Optimization of Integrated Wing-Engine Geometry Using an Unstructured Vorticity Solver," *33rd AIAA Applied Aerodynamics Conference*, AIAA 2015-2880, Dallas, TX, 2015.

[10]Foster, D. N., Ashill, P. R., and Williams, B. R., "The Nature, Development and Effect of the Viscous Flow Around an Aerofoil with High-Lift Devices," CP-1258, Her Majesty's Stationery Office, London, 1974.

[11]Torenbeek, E., *Synthesis of Subsonic Airplane Design*, Kluwer Academic Publishers, Boston, 1982.

[12]Morgan, H. L, Jr. and Paulson, J. W., "Low-Speed Aerodynamic Performance of a High-Aspect-Ratio Supercritical-Wing Transport Model Equipped with Full-Span Slat and Part-Span Double-Slotted Flaps," NASA TP-1580, Dec. 1979.

[13]Morgan, H. L, Jr., "Model Geometry Description and Pressure Distribution Data from Tests of EET High-Lift Research Model Equipped with Full-Span Slat and Part-Span Flaps," NASA TM-80048, Feb. 1979.

[14]Smith, A. M. O., "High-Lift Aerodynamics," *Journal of Aircraft*, Vol. 12, No. 6, 1975, pp. 501–530.